Available online at www.sciencedirect.com

ScienceDirect

Journal of the Franklin Institute 356 (2019) 6160–6174

www.elsevier.com/locate/jfranklin

Fractional order sliding mode control of a pneumatic position servo system

Hai-Peng Ren[a,b,*], Xuan Wang[b], Jun-Tao Fan[b], Okyay Kaynak[a,c,*]

[a] *School of Electronics and Information Engineering, Xi'an Technological University, Xi'an, China*

[b] *Shaanxi Key Laboratory of Complex System Control and Intelligent Information, Xi'an University of Technology, Xi'an, China*

[c] *Department of Electrical and Electronic Engineering, Bogazici University, Istanbul, Turkey*

Received 6 December 2018; received in revised form 2 April 2019; accepted 21 May 2019

Available online 7 June 2019

Abstract

Gas flow has fractional order dynamics; therefore, it is reasonable to assume that the pneumatic systems with a proportional valve to regulate gas flow have fractional order dynamics as well. There is a hypothesis that the fractional order control has better control performance for this inherent fractional order system, although the model used for fractional controller design is integer order. To test this hypothesis, a fractional order sliding mode controller is proposed to control the pneumatic position servo system, which is based on the exponential reaching law. In this method, the fractional order derivative is introduced into the sliding mode surface. The stability of the controller is proven using Lyapunov theorem. Since the pressure sensor is not required, the control system configuration is simple and inexpensive. The experimental results presented indicate the proposed method has better control performance than the fractional order proportional integral derivative (FPID) controller and some conventional integral order control methods. Points to be noticed here are that the fractional order sliding mode control is superior to the integral order sliding mode counterpart, and the FPID is superior to the corresponding integral order PID, both with optimal parameters. Among all the methods compared, the proposed method achieves the highest tracking accuracy. Moreover, the proposed controller has less chattering in the manipulated variable, the energy consumption of the controller is therefore substantially reduced.

* Corresponding authors at: Xi'an Technological University, Xi'an, China.

E-mail addresses: renhaipeng@xaut.edu.cn (H.-P. Ren), 1311408887@qq.com (X. Wang), 5451182@qq.com (J.-T. Fan), okyay.kaynak@boun.edu.tr (O. Kaynak).

https://doi.org/10.1016/j.jfranklin.2019.05.024

1. Introduction

Pneumatic actuators have been widely used in the field of industrial automation. The main advantage of these actuators are their lower costs and larger output power to size ratio [1]. However, they have nonlinearities due to friction force and the complex gas flow across the valve port, dead zone due to stiction force caused by the sealing ring of the cylinder, and weak stiffness due to the compressibility of air. It is therefore difficult to achieve high precision positioning in a pneumatic servo system [2]. As a result, the applications of pneumatic servo systems are conventionally limited to some low precision applications. However, with the development of the high performance to price ratio pneumatic elements (especially, the proportional valve) and the microcontroller (for example, the digital signal processor), the application field of the pneumatic servo systems is extended the area of high precision tracking control.

Currently, many control strategies are introduced into the pneumatic servo system, including PID control [3,4], adaptive backstepping control [5–8], sliding mode control (SMC) [9–16], intelligent control [17–20] etc. Among these methods, SMC is considered to be a more effective way to solve the problems of system uncertainty. For the linear and nonlinear models of pneumatic system, two sliding mode controllers were designed respectively in [9]. However, this method was complex and sensitive to the payload variations. A sliding mode controller was proposed for the pneumatic system with on/off valves and a position feedback in [10], yet this method needed expensive pressure sensor. In [11], an adaptive backstepping SMC method was proposed for pneumatic position servo system. In the design of the controller, the dynamic equations of the system were not required. The controller achieved better tracking performance than the compared methods. However, the stability of the control algorithm is not proven. Due to the discontinuous-input of the pneumatic actuator, a sliding mode controller for an averaged model of pneumatic system is proposed in [12], but in this method, the system model was needed. An adaptive second-order sliding mode output feedback controller was proposed for pneumatic servo system in [13]. Yet the perturbation bound must be known. The derivative of sliding mode variable is not required of this method, and the chattering can be reduced effectively through gain adjustment. A backstepping sliding mode algorithm for independent force-stiffness control of pneumatic cylinders was presented in [14], which achieved good force and stiffness tracking performance. However, the system dynamics are again required in this method. A controller proposed in [15] achieved very good results although the friction was not considered. The controller included a robust motion control loop and a non-linear state feedback pneumatic force control loop. The motion controller was a sliding mode control and the pneumatic dynamics was used as a natural filter of the discontinuous part of the control law. But the chattering of control output is obvious, and expensive pressure sensors are needed. In [16], the use of a reduced order controller was proposed, in which a second order system model with delay input was introduced to design a homogeneous robust nonlinear controller. However, the controller design using the reduced order model are still complicated, and the tracking accuracy improvement is not as good as expected. The sliding surfaces of all aforementioned controllers are the integer order derivative of state (error) variables.

In recent years, fractional order control methods have been widely studied. Different from the integer orders of derivative and integration in conventional calculus, the order of derivative or integration in the fractional order calculus is a real number. In fact, the integer order derivative and integration are special cases of their fractional order counterpart. The fractional

order dynamics were also studied by researchers from different fields [21] including material science, viscoelastic system [22] and extremum seeking application [23]. In particular, fractional order controllers [24–27] have been developed to control some dynamical integer order and fractional order systems. In [28], a fractional order disturbance observer was proposed to estimate the mismatched disturbance, at the same time, a novel fractional order sliding mode controller was proposed based on an observer to decrease the tracking error and the chattering effect. In [29], a fractional order integral slide surface and a switching-type reaching law were introduced in an adaptive SMC, which resulted in less chattering. In [30], a fractional order integral sliding surface was proposed for the stabilization of an uncertain fractional order nonlinear system. In the approach, a fractional order exponential reaching law was used. In [29,30], two proposed methods adopted fractional order integral sliding surface and different reaching laws to reduce the reaching time and then improve the system performance. A sliding surface using fractional order integral was proposed in [31] for the speed control of a permanent magnet synchronous motor in order to reduce the chattering of the controller output and to improve robustness. A sliding surface with a fractional order (larger than 1) derivative term was proposed in [32] to control the attitude of a quad-rotor. A sliding surface with two fractional order derivative terms was proposed in [33] to control a flexible link manipulator robot in order to improve the performance. The approach proposed in this manuscript is different from all the reviewed work in the sense that the use of a sliding surface with one fractional order (less than 1) derivative term is proposed. Furthermore, the proposed method is experimentally verified in pneumatic position servo system.

The pneumatic system involves gas flow. The research has shown that fluid dynamics has fractional order characteristics [22]. In [34], an optimized fractional order PID (FPID) controller is proposed to control the pneumatic system, and the experimental results show that the FPID controller with the optimized parameters has better performance than the integer order PID (IPID) controller with the optimized parameters. In order to further verify the superiority of fractional order controller, in this paper, a fractional order sliding mode control method with an exponential reaching law is proposed, based on the integer model of the pneumatic servo system. In this method, the fractional derivative is introduced in the traditional sliding surface, which take the advantage of the fractional order derivative property to improve the performance without significantly increasing the complexity of implementation. To the best knowledge of the authors, such a sliding surface is reported for the first time. Since during the design of the controller, only the displacement information needs to be known, the proposed controller is simpler to be implemented. The control system is also easy to analyse because only fractional order sliding surface is used. The control system configuration is simple and inexpensive because no pressure sensors are needed. The stability of the controller is proven by using Lyapunov theorem. The experimental results presented indicate that the proposed method achieves better tracking of the reference signals, and less energy consumption as compared to other methods.

This paper is arranged as follows. The description of the linearized mathematical model is given in Section 2. The proposed fractional order sliding mode controller and the proof of system stability are given in Section 3. The experimental comparison results of the proposed method are given in Section 4. The same section includes a comparative analysis of the proposed approach with other methods. A number of conclusions are offered in Section 5.

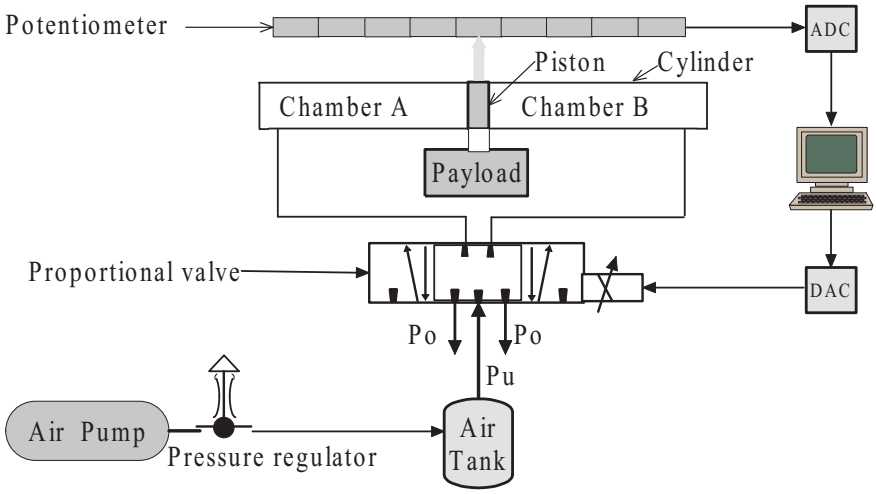

Fig. 1. Schematic diagram of pneumatic position servo system.

2. Mathematical model of pneumatic position servo system

The schematic diagram of the pneumatic position servo system is shown in Fig. 1. The air is compressed by the air pump, and then flows into the Chamber A or B of the cylinder. Due to the difference of air flow rate between Chamber A and Chamber B, the pressure difference across the piston is produced, which drives the piston and payload. The potentiometer detects the position information of the load and sends it to the computer via analog-to-digital conversion (ADC). The designed controller regulates the proportional valve via digital-to-analog conversion (DAC).

The model of the pneumatic position servo system is described as follows [5,6,11]:

$$\begin{cases} \dot{m}_a = f_a(u, p_a) \\ \dot{m}_b = f_b(u, p_b) \\ KRT\dot{m}_a = Kp_aA_a\dot{y} + A_a(y_0 + y)\dot{p}_a \\ KRT\dot{m}_b = -Kp_bA_b\dot{y} + A_b(y_0 - y)\dot{p}_b \\ M\ddot{y} = p_aA_a - p_bA_b - F_f \end{cases}, \tag{1}$$

where, $\dot{m}_a$ and $\dot{m}_b$ are the mass rates of Chambers A and B, respectively. p_a and p_b are pressures in Chambers A and B, A_a and A_b are the intersecting surface area of the two sides of the piston corresponding to Chambers A and B, respectively, y is the payload displacement, y_o is the initial position of the payload, M is the total mass of the payload and piston, F_f is the friction force, K is the adiabatic index of gas, R is ideal gas constant, T is the air temperature, u is the input voltage of the proportional valve and $f_a(u, p_a)$, $f_b(u, p_b)$ are nonlinear functions of the upper stream and the lower stream pressure of Chambers A and B, respectively, which are given as:

$$\begin{cases} f_a(u, p_a) = \sqrt{p_u - p_a}(c_{a_1}u + c_{a_2}u^2) \\ f_b(u, p_b) = \sqrt{p_b - p_0}(c_{b_1}u + c_{b_2}u^2) \end{cases}, \tag{2}$$

where p_u is the downstream or outlet pressure, p_0 is the atmospheric pressure c_{a_1}, c_{a_2}, c_{b_1}, c_{b_2} are constants related to the air property.

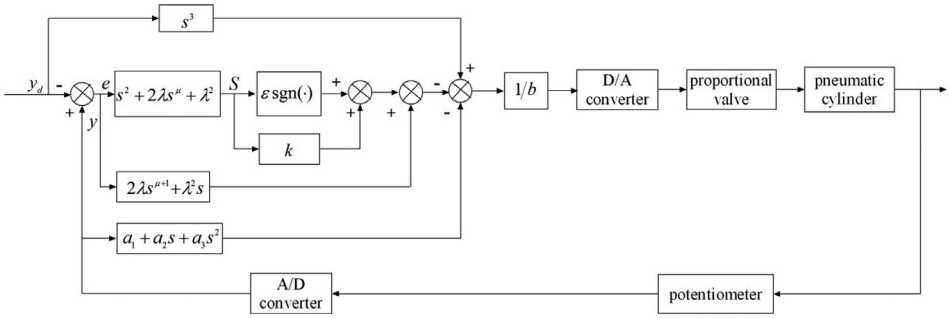

Fig. 2. Block diagram of the fractional order sliding mode control system.

In order to facilitate analysis and system design, $f_a(u, p_a)$ and $f_b(u, p_b)$ are linearized, and the friction F_f and other unmodeled factors are treated as disturbances, then a third-order linear model is derived from Eq. (1) as follows [9]:

$$\dddot{y} = a_1 y + a_2 \dot{y} + a_3 \ddot{y} + bu + d, \tag{3}$$

where a_1, a_2, a_3 and b are the model parameters, d is the disturbance, $|d| \le dis$, dis is a constant.

Define the state variables as $x_1 = y$, $x_2 = \dot{y}$ and $x_3 = \ddot{y}$, which represent the displacement, the velocity and the acceleration of the payload, respectively. The third-order linear model can then be written as:

$$\begin{cases} \dot{x}_1 = x_2 \\ \dot{x}_2 = x_3 \\ \dot{x}_3 = a_1 x_1 + a_2 x_2 + a_3 x_3 + bu + d \\ y = x_1 \end{cases}. \tag{4}$$

It is noted that due to the system structure and other design reasons, it is difficult to get the exact values of the model parameters. Furthermore, the parameters might be time-varying according to the different position of the piston. The linearized model given by Eq. (4) is used for design and analysis of a fractional order controller. Although the model used is integer order, the fractional order designed based on this model achieves very good performance.

3. Fractional order sliding mode controller

3.1. Fractional order sliding mode controller design

The control goal is to make the output y of system (4) track the reference signal y_d asymptotically. The block diagram of the fractional order sliding mode control system is shown in Fig. 2.

The tracking error is defined as $e = y(t) - y_d(t)$. The sliding mode surface is defined as:

$$S = \ddot{e} + 2\lambda D^\mu e + \lambda^2 e, \tag{5}$$

where, $D^\mu e$ is the μ order derivative of the e. The definition of the μ order derivative can be found in [34]. If $\mu = 1$, Eq. (5) is an ordinary sliding mode surface. Here, $1 < \mu < 2$

corresponds a fractional order sliding surface. The time derivative of S is:

$$\dot{S} = \dddot{e} + 2\lambda D^{\mu+1} e + \lambda^2 \dot{e}. \tag{6}$$

The exponential reaching law below is used:

$$\dot{S} = -\epsilon sgn(S) - kS, \tag{7}$$

where $\epsilon > 0$ and $k > 0$ are constants.

From Eqs. (6) and (7), we have:

$$\dddot{e} = (\dddot{y} - \dddot{y}_d) = -\epsilon sgn(S) - kS - 2\lambda D^{\mu+1} e - \lambda^2 \dot{e}. \tag{8}$$

The control law is obtained by Eqs. (4) and (8).

$$u = \frac{1}{b}[-\epsilon sgn(S) - kS - a_1 x_1 - a_2 x_2 - a_3 x_3 + \dddot{y}_d - 2\lambda D^{\mu+1} e - \lambda^2 \dot{e}]. \tag{9}$$

3.2. Stability analysis of the control system

The Lyapunov function is defined as:

$$V = \frac{1}{2} S^2. \tag{10}$$

Then, the time derivative of V is:

$$\begin{aligned} \dot{V} &= S\dot{S} = S(\dddot{e} + 2\lambda D^{\mu+1} e + \lambda^2 \dot{e}) \\ &= S(\dddot{y} - \dddot{y}_d + 2\lambda D^{\mu+1} e + \lambda^2 \dot{e}) \\ &= S(a_1 x_1 + a_2 x_2 + a_3 x_3 + bu + d - \dddot{y}_d + 2\lambda D^{\mu+1} e + \lambda^2 \dot{e}). \end{aligned} \tag{11}$$

Substituting Eq. (9) into Eq. (11), we obtain:

$$\dot{V} = S\dot{S} = S(d - \epsilon sgn(S) - kS) \leqslant -(\epsilon - d)|S| - kS^2. \tag{12}$$

Using the Lyapunov stability theory, we know that by choosing a suitable parameter to ensure $\epsilon > dis$, the system state will asymptotically approach to the sliding surface given by $S = 0$.

When $S = 0$, we have:

$$\ddot{e} + 2\lambda D^{\mu} e + \lambda^2 e = 0. \tag{13}$$

By Laplace transform, the above equation can be expressed as:

$$s^2 E(s) + 2\lambda s^{\mu} E(s) + \lambda^2 E(s) = 0. \tag{14}$$

According to the classical control theory, the above equation can be treated as a close-loop system with e as output and open-loop transfer function given by:

$$G_k(s) = \frac{1}{\lambda^2}(s^2 + 2\lambda s^{\mu}). \tag{15}$$

According to the conclusion in [33], the phase of this open loop transfer function is always greater than $-\pi/2$ and there is no pole in the right half plane. Therefore the Nyquist theorem can be used to prove the stability of the closed-loop system. According to the final-value theorem of the fractional order system Laplace transform we have:

$$\lim_{t \to \infty} e = \lim_{s \to 0} \frac{s}{\lambda^2}(s^2 + 2\lambda s^{\mu}) = 0. \tag{16}$$

To this end, we conclude that the tracking error e tends to zero if S tends to zero, which means that the pneumatic system output can asymptotically track the reference signal.

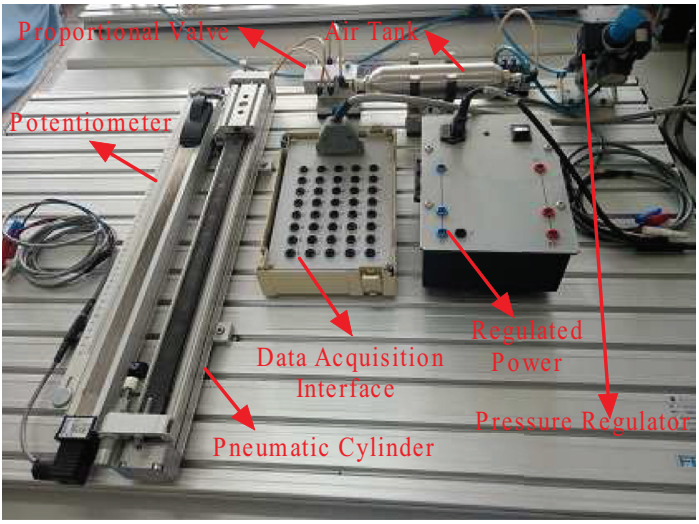

Fig. 3. Photo of the pneumatic servo system.

4. Experimental results and their comparison to existing methods

4.1. Experimental platform

The experimental platform used in this study is manufactured by Festo Company of Germany. It includes a regulated power supply, a rod-less cylinder, a pressure regulator, a potentiometer, a proportional three position five-way valve, a payload and a PCI2306 data acquisition card. The photograph of the experimental equipment photo is shown in Fig. 3.

The software used in the experiment is Visual Basic. The user interface displays the payload position and the reference signals, it is also used to select the type of the input signal, to set the parameters, and so on. The controller output is forced to saturate within the range $[U_{\min}, U_{\max}]$. The sampling time is set to 10ms, the actual position of the payload y is detected by the sensor. Before the experiment, the piston is forced to the middle point of the cylinder.

Reference signals are defined as follows [35]:

(1) Reference signal 1:

$$y_d = A_1 \sin(\omega_1 t), \tag{17}$$

where $A_1 = 167.475,\ \omega_1 = 0.5\pi$.

(2) Reference signal 2:

$$y_d = \begin{cases} -(A_2/\omega_2^2)\sin(\omega_2 t) + (A_2/\omega_2)t, & t < 4 \\ 142.157, & t \geq 4 \end{cases}, \tag{18}$$

where $A_2 = 55.825,\ \omega_2 = 0.5\pi$.

(3) Reference signal 3:

$$\begin{aligned} y_d = {} & A_3[\sin(2\omega_3 t) + \sin(\omega_3 t) + \sin(4\omega_3 t/7) \\ & + \sin(\omega_3 t/3) + \sin(4\omega_3 t/17)], \end{aligned} \tag{19}$$

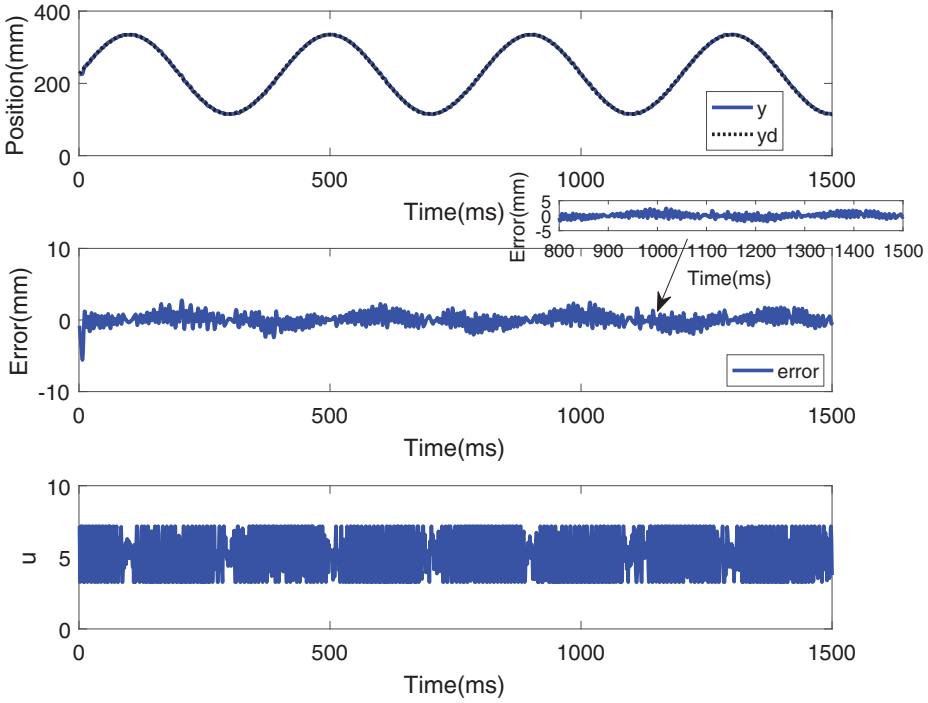

Fig. 4. Experimental results for tracking the sinusoidal signal using integer order SMC. (For interpretation of the references to color in this figure, the reader is referred to the web version of this article.)

where $A_3 = 167.475$, $\omega_3 = 0.5\pi$.

4.2. Experiment results with the conventional sliding mode controller

If $\mu = 1$, Eq. (9) reverses to an integer order sliding mode controller. By doing a system identification, the model parameters of Eq. (4) are roughly obtained as $a_1 = 0$, $a_2 = -218.43$, $a_3 = -29.55$ and $b = 5559.20$. The controller parameters are set to $\lambda = 110$, $\epsilon = 1$, and $k = 185$ (which are finely tuned to obtain the best result). The corresponding experimental results of tracking three reference signals are shown in Figs. 4, 5 and 6, respectively.

In Figs. 4–6, the black dash line is a reference signal, the blue solid line is the actual output of the system in the upper panel. At the same time, the middle panel shows the tracking error, the lower panel of each plot shows the corresponding controller output.

According to Figs. 4–6, we know that the output of the pneumatic position servo system can track the reference signals, however, the controller output oscillates with a relative large amplitude between the upper and the lower limits.

4.3. Experimental results of the proposed method

The controller parameters are set as $\mu = 1.5$, $\lambda = 41$, $\epsilon = 5$, $k = 60$, $h = 0.01$ and $n = 20$ in Eq. (9). The experimental results corresponding to tracking three reference signals are shown in Figs. 7, 8 and 9, respectively.

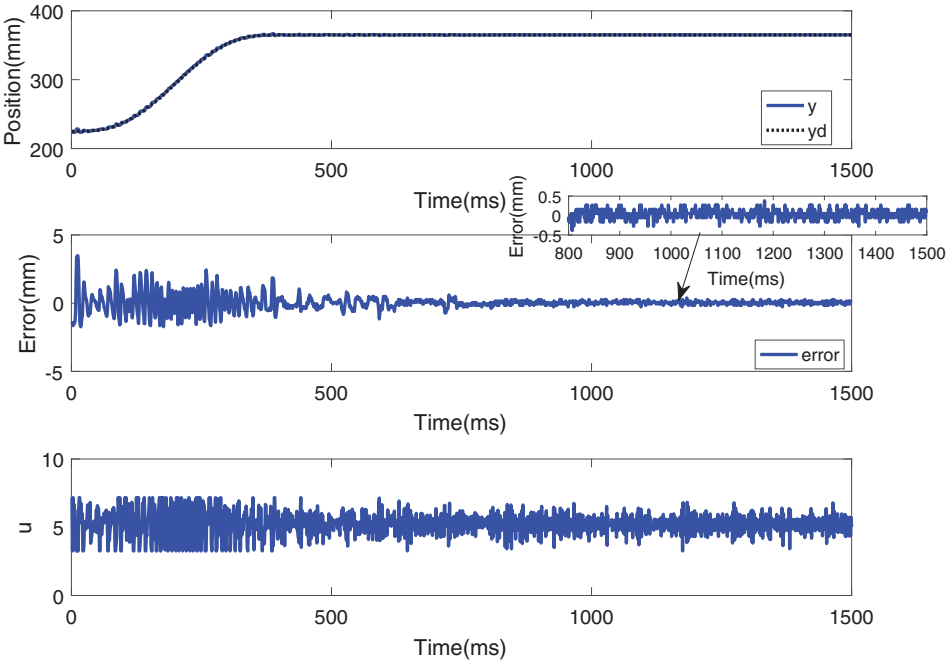

Fig. 5. Experimental results for tracking the s-curve signal using integer order SMC. (For interpretation of the references to color in this figure, the reader is referred to the web version of this article.)

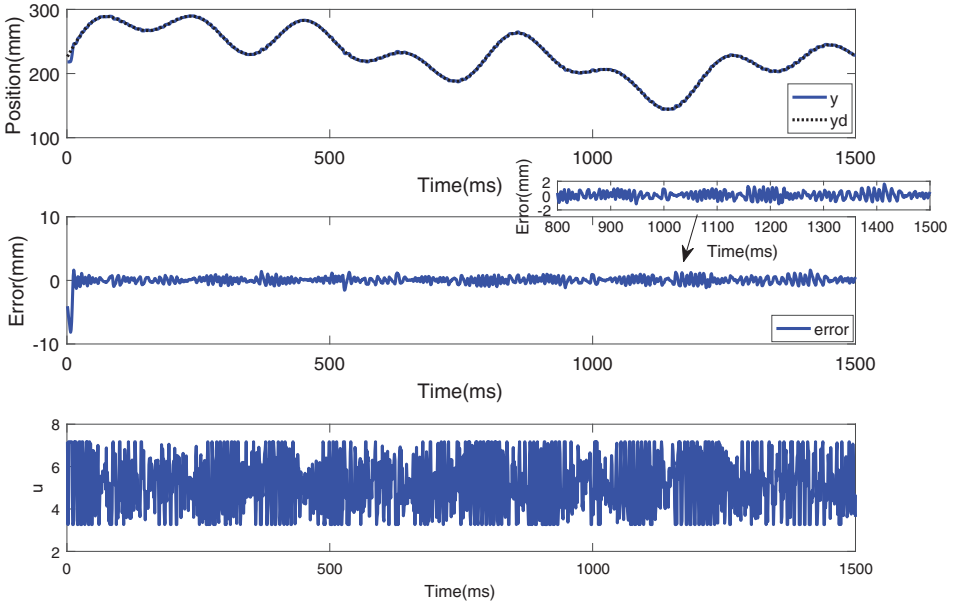

Fig. 6. Experimental results for tracking the multi-frequency sinusoidal signal using integer order SMC. (For interpretation of the references to color in this figure, the reader is referred to the web version of this article.)

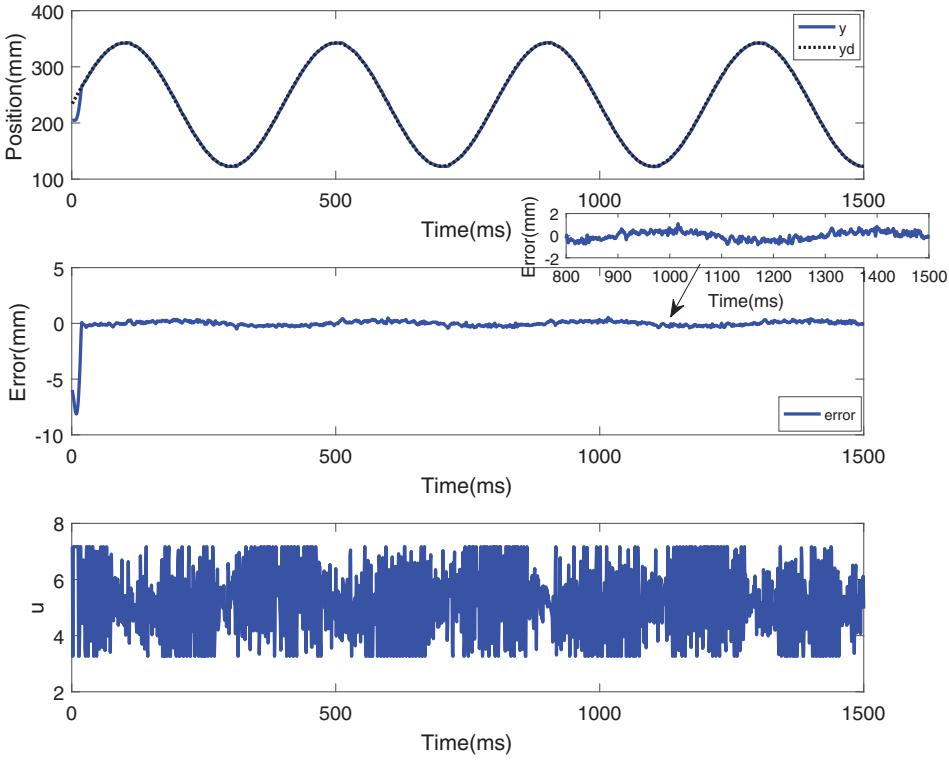

Fig. 7. Experimental results for tracking the sinusoidal signal using the proposed method.

Figs. 7–9 show that the output of the pneumatic position servo system can track the reference signals with higher precision, with relatively small controller output chattering than those of the corresponding integer order SMC.

4.4. Comparison of experimental results

The proposed method is comparised to the methods in [5,6,9–11,34,36–38] for tracking three references, respectively. The corresponding controllers and parameter settings of the method in [5,6,9–11,36] can be found in [34]. The controller parameters in [37] are $a_0 = 5$, $a_1 = 10$, $a_2 = 20$, $k_1 = 1000$, $k_2 = 30$, $\gamma = 800$, $\kappa = 50$, $\nu = 0.01$, $\epsilon = 10$. The controller parameters in [38] are $b = 2000$, $a_0 = 1$, $a_1 = 2$, $a_2 = 100$, $g_0 = 2$, $g_1 = 500$, $h_0 = h_1 = 30$, $q_0 = 9$, $p_0 = 1$, $h_2 = h_3 = 100$, $q_2 = q_3 = 3$, $p_2 = p_3 = 1$. Here, the controller parameter notations might be identical, however, correspond to the description of different papers.

Defining the root mean square error to compare the steady state tracking error of all methods quantitatively, which is given as:

$$RMSE = \sqrt{\frac{1}{N}\sum_{k=N_1}^{N_2} {e_k}^2}, \tag{20}$$

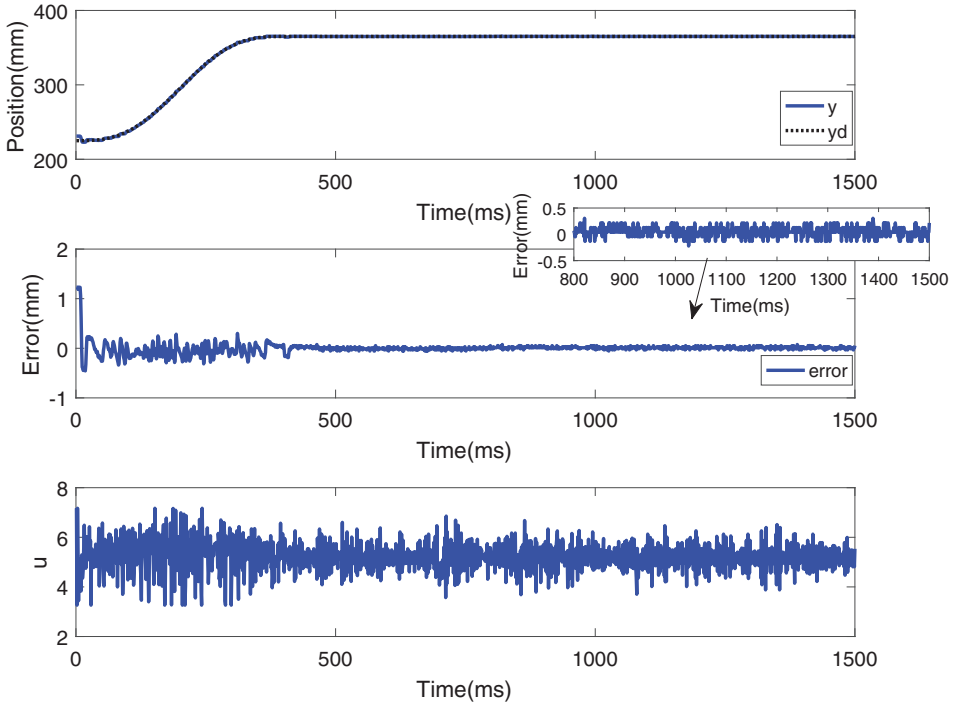

Fig. 8. Experimental results for tracking the s-curve signal using the proposed method.

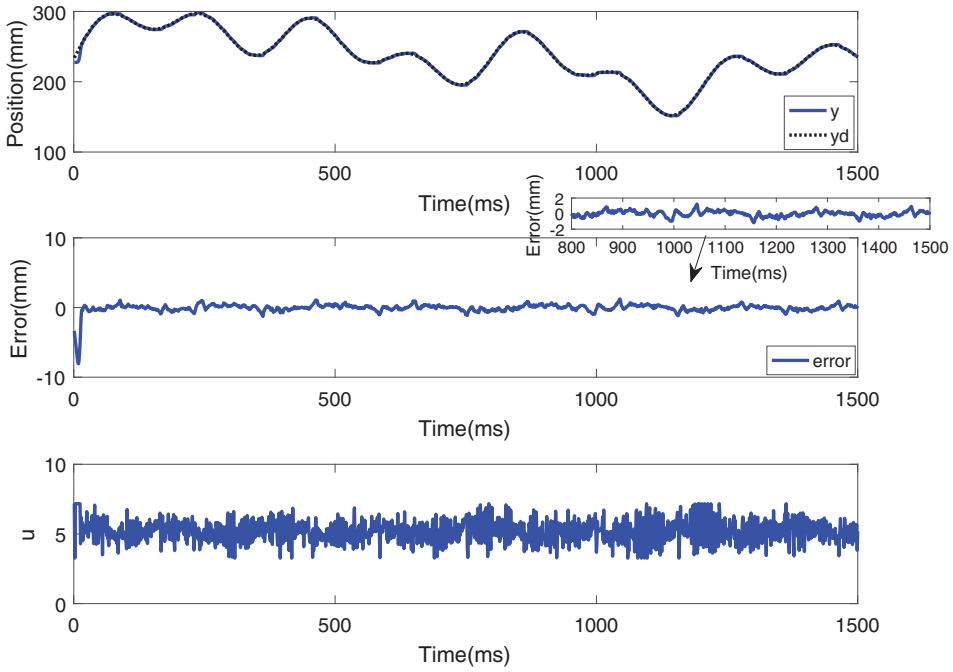

Fig. 9. Experimental results for tracking the multi-frequency sinusoidal signal using the proposed method.

Table 1
RMSE (mm) and Q (v) for ten methods to track the sinusoidal signal.

Methods	Index	Max.	Avg.
Method in [5]	RMSE	2.6057 mm	2.5233 mm
	Q	2930.4 v	2930.4 v
Method in [6]	RMSE	2.4579 mm	2.4249 mm
	Q	2930.4 v	2930.4 v
Method in [9]	RMSE	2.5387 mm	2.5144 mm
	Q	2862.8 v	2858.8 v
Method in [10]	RMSE	2.5034 mm	2.4804 mm
	Q	2930.4 v	2930.4 v
Method in [11]	RMSE	2.0995 mm	2.0350 mm
	Q	2930.4 v	2930.4 v
Optimized IPID in [34]	RMSE	1.0858 mm	1.0589 mm
	Q	2198.6 v	2131.8 v
Optimized FPID in [34]	RMSE	0.7397 mm	0.7108 mm
	Q	1284.9 v	1221.2 v
Integer order SMC in [36]	RMSE	2.0675 mm	2.0416 mm
	Q	2882.2 v	2874.7 v
Super-Twisting SMC in [37]	RMSE	2.0767 mm	2.0285 mm
	Q	1793.7 v	1605.8 v
Terminal SMC in [38]	RMSE	2.6137 mm	2.2807 mm
	Q	1466.0 v	1465.9 v
Proposed method	RMSE	1.0368 mm	1.0148 mm
	Q	1074.4 v	1037.1 v

where $N = N_2 - N_1$, N_1 represents the start time of consideration, N_2 represents the end time of consideration. e_k is the tracking error at kth sampling time defined by $e_k = y_d(kT) - y(kT)$, where T is the sampling time.

For comparing energy consumption of different control methods quantitatively, energy consumption Q is defined as

$$Q = \sum_{k=N_1}^{N_2} |u_k - u_0|, \tag{21}$$

where, u_k is the control voltage value at kth time sampling, u_0 is the zero point of the proportional valve.

To reduce the effect of noise and initial conditions, each experiment was carried out thirty times to get average *RMSE*, max *RMSE*, average Q, and max Q. The quantitative comparison results are shown in Tables 1, 2, 3 for three reference signals, respectively.

According to Tables 1–3, we conclude that the *RMSE* of the proposed method is less than those of other methods, and the energy consumption of the proposed method is the least one. Controller designed in this paper has better tracking performance than some existing methods. This is another evidence that a fractional order controller should be expected to performance better than the integer order counterpart for a plant that possibly has fractional order dynamics.

Table 2
RMSE (mm) and Q (v) for ten methods to track the s-curve signal.

Methods	Index	Max.	Avg.
Method in [5]	RMSE	0.8955 mm	0.8759 mm
	Q	2930.4 v	2930.4 v
Method in [6]	RMSE	0.8700 mm	0.8147 mm
	Q	2930.4 v	2930.4 v
Method in [9]	RMSE	0.9620 mm	0.9359 mm
	Q	2900.6 v	2904.1 v
Method in [10]	RMSE	0.9730 mm	0.9261 mm
	Q	2930.4 v	2930.4 v
Method in [11]	RMSE	0.6263 mm	0.6051 mm
	Q	2930.4 v	2930.4 v
Optimized IPID in [34]	RMSE	0.3291 mm	0.2977 mm
	Q	1346.2 v	1230.5 v
Optimized FPID in [34]	RMSE	0.3145 mm	0.2640 mm
	Q	909.1 v	874.4 v
Integer order SMC in [36]	RMSE	0.6763 mm	0.6502 mm
	Q	2783.8 v	2768.4 v
Super-Twisting SMC in [37]	RMSE	0.6999 mm	0.5955 mm
	Q	1595.0 v	1594.3 v
Terminal SMC in [38]	RMSE	0.9564 mm	0.8251 mm
	Q	1466.4 v	1466.4 v
Proposed method	RMSE	0.2604 mm	0.2248 mm
	Q	687.9 v	685.9 v

Table 3
RMSE (mm) and Q (v) for ten methods to track the multi-frequency sinusoidal signal.

Methods	Index	Max.	Avg.
Method in [5]	RMSE	1.2594 mm	1.2217 mm
	Q	2930.4 v	2930.4 v
Method in [6]	RMSE	1.3250 mm	1.2411 mm
	Q	2930.4 v	2930.4 v
Method in [9]	RMSE	1.3827 mm	1.3316 mm
	Q	2921.8 v	2911.3 v
Method in [10]	RMSE	1.3368 mm	1.3059 mm
	Q	2930.4 v	2930.4 v
Method in [11]	RMSE	1.0496 mm	1.0414 mm
	Q	2930.4 v	2930.4 v
Optimized IPID in [34]	RMSE	0.6781 mm	0.6288 mm
	Q	1644.3 v	1598.5 v
Optimized FPID in [34]	RMSE	0.6023 mm	0.5739 mm
	Q	1031.9 v	1010.6 v
Integer order SMC in [36]	RMSE	1.1059 mm	1.0661 mm
	Q	2848.5 v	2840.7 v
Super-Twisting SMC in [37]	RMSE	1.1142 mm	1.0445 mm
	Q	1701.8 v	1400.9 v
Terminal SMC in [38]	RMSE	1.2857 mm	1.1193 mm
	Q	1466.1 v	1466.1 v
Proposed method	RMSE	0.8309 mm	0.8101 mm
	Q	839.7	832.3 v

5. Conclusion

In this work, a new fractional order sliding mode controller is proposed for experimental control of pneumatic position servo system. The main contributions of this paper are as follows: first, the proposed fractional order sliding mode controller uses a simple fractional order sliding surface for the first time, and the stability of the proposed controller is proved. Second, as compared to the integer order sliding mode control counterpart in the same situation, the proposed controller achieves better performance. Third, according to the experimental results, the proposed method has better performance than some existing methods, moreover, the proposed method reduces the chattering of the control force significantly, and consumes less energy. Finally, since the pressure sensor is not required, the control system structure is simple and inexpensive.

The work in this paper supports the hypothesis given in this paper, at least, for this pneumatic servo system. At the same time, it might indicate that the pneumatic servo system is a fractional order system.

References

[1] A. Llchmann, O. Sawodny, S. Trenn, Pneumatic cylinders: modelling and feedback force-control, Int. J. Control 79 (6) (2005) 650–661, doi:10.1080/00207170600645875.
[2] S. Das, B. Bandyopadyay, A.K. Paul, A. Chalanga, Position control of pneumatic actuator using multi-rate output feedback sliding mode control, in: Proceedings of the IEEE ICECE Conference, Dhaka, Bangladesh, 2012, pp. 920–924, doi:10.1109/ICECE.2012.6471701.
[3] R.B. Varseceld, G.M. Bone, Accurate position control of a pneumatic actuator using on/off solenoid valves, IEEE/ASME Trans. Mechatron. 3 (2) (1977) 195–204, doi:10.1109/3516.622972.
[4] M. Taghizadeh, F. Najafi, A. Ghaffari, Multimodel PD-control of a pneumatic actuator under variable loads, Int. J. Adv. Manufact. Technol. 48 (5–8) (2010) 655–662, doi:10.1007/s00170-009-2293-3.
[5] H.P. Ren, C. Huang, Experimental tracking control for pneumatic system, in: Proceedings of the IEEE IECON Conference, Vienna, Austria, 2013, pp. 4124–4129, doi:10.1109/IECON.2013.6699797.
[6] H.P. Ren, C. Huang, Adaptive backstepping control of pneumatic servo system, in: Proceedings of the IEEE Symposium on ISIE, Taibei, 2013, pp. 1–6, doi:10.1109/ISIE.2013.6563773.
[7] A. Boubakir, F. Plestan, S. Labiod, F. Boudjema, A stable linear adaptive controller applied to a pneumatic actuator system, in: Proceedings of the IEEE Decision and Control Conference, Florence, Italy, 2013, pp. 6112–6117, doi:10.1109/CDC.2013.6760855.
[8] D.Y. Meng, G.L. Tao, X.C. Zhu, Integrated direct/indirect adaptive robust motion trajectory tracking control of pneumatic cylinders, Int. J. Control 86 (9) (2013) 1620–1633, doi:10.1080/00207179.2013.792002.
[9] G.M. Bone, S. Ning, Experimental comparison of position tracking control algorithms for pneumatic cylinder actuators, IEEE/ASME Trans. Mechatron. 12 (5) (2007) 557–561, doi:10.1109/TMECH.2007.905718.
[10] T. Nguyen, J. Leavitt, F. Jabbari, J.E. Bobrow, Accurate slide-mode control of pneumatic systems using low-cost solenoid valves, IEEE/ASME Trans. Mechatron. 12 (2) (2007) 216–219, doi:10.1109/TMECH.2007.892821.
[11] H.P. Ren, J.T. Fan, Adaptive backstepping sliding mode control of pneumatic position servo system, Chin. J. Mech. Eng. 29 (5) (2016) 1003–1009, doi:10.3901/CJME.2016.0412.050.
[12] S. Hodgson, M. Tavakolt, M.T. Pham, A. Leleve, Nonlinear discontinuous dynamics averaging and PWM-based sliding control of solenoid-valve pneumatic actuators, IEEE/ASME Trans. Mechatron. 20 (2) (2015) 876–888, doi:10.1109/TMECH.2014.2326601.
[13] A. Estrada, F. Plestan, Second order sliding mode output feedback control with switching gains-application to the control of a pneumatic actuator, J. Frankl. Inst. 351 (4) (2014) 2335–2355, doi:10.1016/j.jfranklin.2013.07.011.
[14] B. Taheri, D. Case, E. Richer, Force and stiffness backstepping sliding mode controller for pneumatic cylinders, IEEE/ASME Trans. Mechatron. 19 (6) (2014) 1799–1809, doi:10.1109/TMECH.2013.2294970.
[15] J.F. Carneiro, F.G.D. Almeida, Accurate motion control of a servo pneumatic system using integral sliding mode control, Int. J. Adv. Manufact. Technol. 77 (9–12) (2015) 1533–1548, doi:10.1007/s00170-014-6518-8.

[16] E. Edjekouane, S. Riachy, M. Ghanes, J.P. Barbot, Robust control of pneumatic actuators based on a simplified model with delayed input, in: Proceedings of the IEEE ICECE Conference, Nantes, France, 2014, pp. 1–6, doi:10.1109/VSS.2014.6881117.
[17] L. Thananchai, Fuzzy logic based PWM control and neural controlled-variable estimation of pneumatic artificial muscle actuators, Expert Syst. Appl. 38 (6) (2011) 7837–7850, doi:10.1016/j.eswa.2010.12.120.
[18] N. Garmsiri, N. Sepehri, Emotional learning based position control of pneumatic actuators, Expert Syst. Appl. 20 (3) (2014) 433–450, doi:10.1080/10798587.2014.901651.
[19] B. Dehghan, B.W. Surgenor, Comparison of fuzzy and neural network adaptive methods for the position control of a pneumatic system, in: Proceedings of the IEEE Canadian Computer Engineering Conference, Regina, Saskatchewan, Canada, 2013, pp. 1–4, doi:10.1109/CCECE.2013.6567712.
[20] J.F. Carneiro, F.G.D. Almeida, A high-accuracy trajectory following controller for pneumatic devices, Int. J. Adv. Manufact. Technol. 61 (1–4) (2012) 253–267, doi:10.1007/s00170-011-3695-6.
[21] H.S. Ahn, Y.Q. Chen, I. Podlubny, Robust stability test of a class of linear time-invariant interval fractional-order system using Lyapunov inequality, Expert Syst. Appl. 187 (1) (2007) 27–34, doi:10.1016/j.amc.2006.08.099.
[22] J.L. Battaglia, J.C. Batsale, L.L. Lay, A. Oustaloup, O. Cois, Heat flow estimation through inverted non-integer identification model, Int. J. Therm. Sci. 39 (3) (2000) 374–389.
[23] C. Yin, X. Huang, S. Dadras, Y. Cheng, J. Cao, H. Malek, J. Mei, Design of optimal lighting control strategy based on multi-variable fractional-order extremum seeking method, Info. Sci. 465 (2018) 38–C60, doi:10.1016/j.ins.2018.06.059.
[24] I. Podlubny, Fractional-order systems and $PI^{\lambda}D^{\mu}$ controllers I, IEEE Trans. Autom. Control 44 (1) (1999) 208–214, doi:10.1109/9.739144.
[25] H.F. Raynaud, A. Zergainoh, State-space representation for fractional order controllers, Automatica 36 (7) (2000) 1017–1021, doi:10.1016/s0005-1098(00)00011-x.
[26] K. Erenturk, Fractional-order and active disturbance rejection control of nonlinear two-mass drive system, IEEE Trans. Indust. Electron. 60 (9) (2013) 3806–3813, doi:10.1109/TIE.2012.2207660.
[27] L.F. Chen, D.Y. Xue, Simulation of fractional order control based on IPMC model, in: Proceedings of the Chinese Control and Decision Conference, Qingdao, China, 2014, pp. 598–601, doi:10.1109/CCDC.2014.6852236.
[28] J. Wang, C.F. Shao, Y.Q. Chen, Fractional order sliding mode control via disturbance observer for a class of fractional order systems with mismatched disturbance, Mechatronics 53 (2018) 8–19, doi:10.1016/j.mechatronics.2018.05.006.
[29] C. Yin, Y.H. Cheng, Y.Q. Chen, B. Stark, S.M. Zhong, Adaptive fractional-order switching-type control method design for 3d fractional-order nonlinear systems, Nonlinear Dyn. 82 (1–2) (2015) 39–52, doi:10.1007/s11071-015-2136-8.
[30] C. Yin, X.G. Huang, Y.Q. Chen, S. Dadras, S.M. Zhong, Y.H. Cheng, Fractional-order exponential switching technique to enhance sliding mode control, Appl. Math. Model. 44 (2017) 705–726, doi:10.1016/j.apm.2017.02.034.
[31] W.B. Zhang, Z.C. Miao, X.F. Yu, T.L. Han, Fractional order integral sliding mode control for permanent magnet synchronous motor based on improved sliding mode observer, Electr. Mach. Control Appl. 45 (7) (2018) 8–14, doi:CNKI:SUN:ZXXD.0.2018-07-002.
[32] Y.N. Guo, Z.S. Deng, L.Y. Zu, Y.Y. Lv, Trajectory tracking control of a quad-rotor using fractional-order sliding mode, in: Proceedings of the Thirty-sixth Chinese Control Conference, Dalian, China, 2017, pp. 6414–6419, doi:10.23919/ChiCC.2017.8028375.
[33] H. Delavari, P. Lanusse, J. Sabatier, Fractional order controller design for a flexible link manipulator robot, Asian J. Control 15 (3) (2013) 783–795, doi:10.1002/asjc.677.
[34] H.P. Ren, J.T. Fan, O. Kaynak, Optimal design of a fractional order PID controller for a pneumatic position servo system, IEEE Trans. Indust. Electron. 66 (8) (2019) 6220–6229, doi:10.1109/TIE.2018.2870412.
[35] H.P. Ren, X. Wang, PLC based variable structure control of hydraulic position servo system considering controller saturation, in: Proceedings of the thirteenth IEEE Conference on Industrial Electronics and Applications, Wuhan, China, 2018, pp. 135–140, doi:10.1109/ICIEA.2018.8397703.
[36] M. Bouri, D. Thomasset, Sliding control of an electropneumatic actuator using an integral switching surface, IEEE Trans. Control Syst. Technol. 9 (2) (2001) 368–375, doi:10.1109/87.911388.
[37] Y. Shtessel, M. Taleb, F. Plestan, A novel adaptive-gain supertwisting sliding mode controller: Methodology and application, Automatica 48 (5) (2012) 759–769, doi:10.1016/j.automatica.2012.02.024.
[38] C.S. Chiu, Derivative and integral terminal sliding mode control for a class of MIMO nonlinear systems, Automatica 48 (2) (2012) 316–326, doi:10.1016/j.automatica.2011.08.055.